

# Inhibition of Kpn $\beta$ 1 Mediated Nuclear Import Enhances Cisplatin Chemosensitivity in Cervical Cancer.

**Ru-pin Alicia Chi**

University of Cape Town

**Pauline van der Watt**

University of Cape Town

**Wei Wei**

Pfizer Global Pharmaceuticals: Pfizer Inc

**Michael Birrer**

University of Arkansas for Medical Sciences

**Vima Leaner** (✉ [vima.leaner@uct.ac.za](mailto:vima.leaner@uct.ac.za))

University of Cape Town <https://orcid.org/0000-0002-0417-8610>

---

## Research article

**Keywords:** cisplatin, INI-43, nuclear import, p53, NF $\kappa$ B, cervical cancer

**Posted Date:** September 28th, 2020

**DOI:** <https://doi.org/10.21203/rs.3.rs-78192/v1>

**License:**  This work is licensed under a Creative Commons Attribution 4.0 International License.

[Read Full License](#)

---

**Version of Record:** A version of this preprint was published on February 2nd, 2021. See the published version at <https://doi.org/10.1186/s12885-021-07819-3>.

# Abstract

**Background:** Inhibition of nuclear import via Karyopherin beta 1 (Kpn $\beta$ 1) shows potential as an anti-cancer approach. This study investigated the use of nuclear import inhibitor, INI-43, in combination with cisplatin.

**Methods:** Cervical cancer cells were pre-treated with INI-43 before treatment with cisplatin, and MTT cell viability and apoptosis assays performed. Activity and localisation of p53 and NF $\kappa$ B was determined after co-treatment of cells.

**Results:** Pre-treatment of cervical cancer cells with INI-43 at sublethal concentrations enhanced cisplatin sensitivity, evident through decreased cell viability and enhanced apoptosis. Kpn $\beta$ 1 knock-down cells similarly displayed increased sensitivity to cisplatin. Combination index determination using the Chou-Talalay method revealed that INI-43 and cisplatin engaged in synergistic interactions. p53 was found to be involved in the cell death response to combination treatment as its inhibition abolished the enhanced cell death observed. INI-43 pre-treatment resulted in moderately stabilized p53 and induced p53 reporter activity, which translated to increased p21 and decreased Mcl-1 upon cisplatin combination treatment. Furthermore, cisplatin treatment led to nuclear import of NF $\kappa$ B, which was diminished upon pre-treatment with INI-43. NF $\kappa$ B reporter activity and expression of NF $\kappa$ B transcriptional targets, cyclin D1, c-Myc and XIAP, showed decreased levels after combination treatment compared to single cisplatin treatment and this associated with enhanced DNA damage.

**Conclusions:** Taken together, this study shows that INI-43 pre-treatment significantly enhances cisplatin sensitivity in cervical cancer cells, mediated through stabilization of p53 and decreased nuclear import of NF $\kappa$ B. Hence this study suggests the possible synergistic use of nuclear import inhibition and cisplatin to treat cervical cancer.

## Background

Multiple members of the nucleo-cytoplasmic transport system are known to be overexpressed in various cancers (1, 2). We and others have found that siRNA-mediated inhibition of either Chromosome Region Maintenance 1 (Crm1) or Karyopherin Beta 1 (Kpn $\beta$ 1) leads to cancer cell death whilst non-cancer cells are minimally affected, raising the possibility of targeting these proteins as an anti-cancer therapeutic strategy(1).

CRM1 is a nuclear exportin which facilitates nuclear exit of proteins and RNAs(3), and in recent years has received ample attention as a target for cancer treatment(2). Studies have yielded promising results in different cancer models both *in vitro* and *in vivo*(2), with some Crm1 inhibitors currently in clinical trial(4). Kpn $\beta$ 1, on the other hand, is a nuclear importin which transports cargoes from the cytoplasm into the nucleus during interphase(5). In dividing cells, Kpn $\beta$ 1 becomes involved in mitotic processes including regulation of spindle assembly and mitotic exit(6, 7), with its inhibition displaying broad-spectrum anti-cancer effects(1, 8, 9). Using the cervical cancer model, we previously demonstrated that Kpn $\beta$ 1 inhibition

via siRNA led to a G2/M cell cycle arrest coupled with various mitotic defects, which ultimately triggered apoptosis via the intrinsic mitochondrial pathway(10). In search of chemical compounds with inhibitory effects on Kpn $\beta$ 1 function, we previously performed an *in silico* screen and identified a small molecule, Inhibition of Nuclear Import-43 (INI-43), with inhibitory effects on known Kpn $\beta$ 1 cargoes including NFAT, NF $\kappa$ B and AP1(11). Additionally, INI-43 reduced cervical and oesophageal tumour growth in xenograft mouse models(11). Overexpression of Kpn $\beta$ 1 reversed the nuclear import inhibitory effect of INI-43 on NF $\kappa$ B, as well as rescued cells from INI-43-induced death, confirming that INI-43 exerts its effects via interfering with Kpn $\beta$ 1 function(11).

In this study, we addressed the use of INI-43 in combination treatment (CT), by investigating its combined use with a clinically relevant chemotherapeutic agent – cisplatin. CT can be an effective way for treating cancer when participating agents engage in synergism, where the combined use produces greater anti-cancer effects compared to the additive effects of each when used individually. Successful combination chemotherapy translates into longer survival periods for cervical cancer patients, and this has been demonstrated for various combinations including topotecan, irinotecan, gemcitabine and docetaxel when paired with platinum based drugs(12–15). More recently, various natural-derived compounds have been shown to synergize with cisplatin in treating cervical cancer, such as melatonin, epigallocatechin gallate, and genistein *in vitro*(16–18). These findings suggest that platinum-based drugs hold great potential in combinational use. There is also evidence suggesting that interfering with the nuclear transport system could mediate sensitivity to chemotherapeutic agents. Kpn $\beta$ 1 has been reported to confer docetaxel resistance, and siRNA mediated inhibition enhanced the cancer killing effect of docetaxel(19). Furthermore, Kpn $\beta$ 1 overexpression has been shown to enhance the anti-cancer effects of cisplatin (20). The combination of CRM1 inhibition and various conventional chemotherapeutic agents have also yielded promising results in reversing the chemo-resistance of many cancers(21–23), suggesting that manipulating nuclear transport may be a viable option in combination therapy. Selinexor, in particular, reduces the expression of DNA damage repair proteins and potentiates DNA damage-based therapy, including cisplatin(24).

Here we report that the combined use of nuclear import inhibitor INI-43 and cisplatin exhibited synergistic anti-cancer effects in cervical cancer cells. Furthermore, we show that enhanced cell death is mediated through p53 and NF $\kappa$ B function. The advantage of incorporating INI-43 into routine cisplatin use in treating cancer could be beneficial in two ways; firstly, to increase treatment response in patients exhibiting moderate resistance to cisplatin, and secondly, to achieve the same treatment outcome at lower doses of cisplatin, thereby minimizing undesired side effects associated with cisplatin.

## Methods

### Cell lines and tissue culture

HeLa, SiHa, CaSki and C33A cell lines were purchased from the American Type Culture Collection (ATCC) and maintained in Dulbecco's Modified Eagle's Medium (DMEM, Gibco, Life Technologies) containing

10% Fetal Bovine Serum (Gibco, Life Technologies), supplemented with 100 U/mL penicillin and 100 µg/mL streptomycin. Cells were cultured at 37°C in a humidified chamber with 5% CO<sub>2</sub>. All cell lines were authenticated by DNA profiling using the Cell ID System (Promega, Madison, WI, USA).

## Half inhibitory concentration (IC<sub>50</sub>) determination

Cells were plated in 96-well plates and subjected to single or CT (2 hours INI-43 pre-treatment followed by cisplatin treatment, without removing INI-43 from the media) for 48 hours. Following treatment, MTT (Sigma) was added and 4 hours later crystals solubilized using 10% SLS in 0.01 M HCl. Absorbencies were measured at 595 nm and IC<sub>50</sub> values determined via plotting [Fa/(1-Fa)] in log scale against log cisplatin concentration, where  $Fa = \frac{100 - \% \text{ viable cells relative to the untreated}}{100}$ . The half inhibitory concentration was calculated using the formula  $IC_{50} = 10^{x-\text{intercept}}$ .

## Caspase-3/7 assay

Cells were subjected to single or CT for 48 hours, and caspase-3/7 activity monitored using the Promega Caspase-Glo<sup>R</sup> 3/7 assay, according to the manufacturer's instructions. Luminescence was measured using the Veritas™ microplate luminometer (Promega) and results standardized to viable cells in each treatment as determined by MTT assays performed in parallel.

## Combination Index (CI) determination

To elucidate the nature of the combined use of INI-43 and cisplatin, the Chou-Talalay method was adopted(25). Cell viability was determined after 48-hour treatment at fixed INI-43 to cisplatin ratios of 1:3, 1:4 and 1:5 (Table S1). Cell viability was converted to fraction affected (Fa) and CI calculated using CompuSyn software (ComboSyn, Inc.).

## siRNA transfection

Cells were transfected using Transfectin (Bio-Rad) and 20 nM si-Kpnβ1 (H-7, sc-35736, Santa Cruz) or 30 nM si-p53 (sc-29435, Santa Cruz). Control cells were transfected with the equivalent amount of ctrl siRNA (si-ctrl, sc-37007, Santa Cruz).

## Western blot analysis

For protein extraction, cells were washed with PBS and lysed using RIPA buffer (50 mM Tris-Cl, pH7.4, 150 mM NaCl, 1% (w/v) sodium deoxycholate, 0.1% (v/v) SDS, 1% (v/v) Triton X-100, 2 mM EGTA, 2 mM EDTA, 50 mM NaF, 5 mM Na<sub>2</sub>P<sub>2</sub>O<sub>7</sub>, 1 X complete protease inhibitor cocktail (Roche) and 0.1 M Sodium Orthovanadate). For PARP cleavage analysis, dead cells were collected by centrifugation and combined with live cell lysates. Lysates were sonicated, centrifuged, and the supernatant quantified using the BCA Protein Assay Kit (Pierce, Thermo Scientific) according to the manufacturer's instructions. For protein extraction, cells were washed with PBS and lysed using RIPA buffer (50 mM Tris-Cl, pH 7.4, 150 mM NaCl, 1% (w/v) sodium deoxycholate, 0.1% (v/v) SDS, 1% (v/v) Triton X-100, 2 mM EGTA, 2 mM EDTA, 50 mM NaF, 5 mM Na<sub>2</sub>P<sub>2</sub>O<sub>7</sub>, 1 X complete protease inhibitor cocktail (Roche) and 0.1 M Sodium

Orthovanadate). For Parp cleavage analysis, dead cells were collected by centrifugation and combined with live cell lysates. Lysates were sonicated, centrifuged, and the supernatant quantified using the BCA Protein Assay Kit (Pierce, Thermo Scientific) according to the manufacturer's instructions. Proteins were subjected to Western blot analysis using the following antibodies: rabbit anti-Kpn $\beta$ 1 (H-300, sc-11367, Santa Cruz), rabbit anti- $\beta$ -tubulin (H-235, sc-9104, Santa Cruz), rabbit anti-PARP1/2 antibody (H-250, sc-7150, Santa Cruz), mouse anti-GAPDH (0411, sc-47724, Santa Cruz), rabbit anti-p21 (H-164, sc-756, Santa Cruz), rabbit anti-Mcl-1 (H-260, sc-20679, Santa Cruz), mouse anti-cyclin D1 (HD11, sc-246, Santa Cruz), rabbit anti-c-Myc (N-262, sc-764, Santa Cruz), mouse anti-p53 (DO-7, M7001, DakoCytomation), mouse anti-XIAP (610763, BD Biosciences), and rabbit anti-phospho-Histone H2AX ( $\gamma$ H2AX, Ser139, 20E3, #9718, Cell Signal).

## Nuclear/cytoplasmic fractionation

For nuclear/cytoplasmic protein extraction, cells were collected by trypsinization. Cell pellets were resuspended in 10 mM HEPES (pH7.9), 50 mM NaCl, 0.5 M sucrose, 0.1 mM EDTA and 0.5% Triton X-100, followed by centrifugation at 1,000 X G for 10 minutes to separate cytoplasmic (supernatant) and nuclear fractions (pellet). Cytoplasmic fractions were centrifuged at 14,000 X G for 15 minutes at 4<sup>o</sup>C, and the supernatant stored at -80<sup>o</sup>C. Nuclear pellets were washed in 10 mM HEPES, 10 mM KCl, 0.1 mM EDTA and 0.1 mM EGTA, and centrifuged at 1,000 X G for 5 minutes. Pellets were then resuspended in 10 mM HEPES (pH7.9), 500 mM NaCl, 0.1 mM EDTA, 0.1 mM EGTA and 1% (v/v) NP-40 and vortexed for 15 minutes at 4<sup>o</sup>C to extract the nuclear protein, followed by centrifugation at 14,000 X G for 10 minutes. The fractions were quantified using the BCA Protein Assay Kit (Pierce, Thermo Scientific) according to the manufacturer's instructions, followed by western blot analysis.

## p53 half-life ( $T_{1/2}$ ) determination

Cells were treated with 5  $\mu$ M INI-43 or DMSO for two hours or transfected with 20 nM si-ctrl or si-Kpn $\beta$ 1 for 48 hours prior to p53 half-life determination. Cells were treated with 50  $\mu$ g/mL cycloheximide (CHX), and protein harvested at 0, 15, 30, 45, 60 and 90 minutes after CHX treatment. p53 content was analysed by western blotting. Bands were quantified by densitometrical scanning using ImageJ, normalised to GAPDH and expressed as a value relative to p53 intensity at time 0. Relative band intensities were plotted in log scale against time of CHX treatment and a linear trendline drawn. The half-life was calculated using the formula  $T_{1/2}$  (minutes) =  $\text{Log}(2)/[\text{slope}]$ .

## Immunofluorescence

SiHa cells were plated on glass coverslips and treated for 24 hours before fixation with 4% paraformaldehyde. Cells were permeabilised using 0.5% Triton-X-100/PBS and blocked using 1% BSA/PBST with 0.3 M Glycine. Primary antibody incubations were performed in 1% BSA/PBST, followed by secondary antibody incubation (Cy3 conjugated goat anti-rabbit, Jackson ImmunoResearch). Cell nuclei were counterstained with 0.5  $\mu$ g/mL DAPI, and images captured using the Zeiss inverted fluorescence microscope under 100 X oil immersion.

# Luciferase reporter assay

SiHa cells were transfected with 100 ng p65-luciferase reporter construct (containing five copies of the p65-binding site, Promega) or 200 ng p53-luciferase reporter construct (containing thirteen wildtype p53 binding sites, Addgene plasmid #16442, Addgene Plasmid Repository(26) and 10 ng pRL-TK (encoding Renilla luciferase, Promega), using Genecellin transfection reagent (Celtic Molecular Diagnostics). The following day cells were treated with 5  $\mu$ M INI-43 for 2 hours, followed by 30  $\mu$ M cisplatin for 24 hours, and luciferase activity assayed using the Dual-Luciferase Report assay system (Promega), according to the manufacturer's instructions. Luciferase readings were measured using the Veritas™ microplate luminometer (Promega) and normalised to Renilla luciferase from the same extract.

## Statistical analysis

For all data comparisons, the Student's t test was performed using Microsoft Excel. A p value of < 0.05 was considered statistically significant.

## Results

### INI-43 pre-treatment enhanced HeLa and SiHa cell sensitivity to cisplatin

To investigate whether nuclear import inhibition could influence cancer cell sensitivity to cisplatin treatment, cisplatin IC<sub>50</sub> values were compared between cervical cancer cells with and without INI-43 pre-treatment. Pre-treatment was conducted at sublethal INI-43 concentrations ( $\leq 10 \mu$ M) for 2 hours (concentrations which were previously shown to reduce nuclear import of various Kpn $\beta$ 1 cargoes(11)), followed by cisplatin treatment. Cisplatin IC<sub>50</sub> values after 48-hour treatments were 18.0  $\mu$ M, 18.1  $\mu$ M, 30.8  $\mu$ M and 12.8  $\mu$ M for HeLa, CaSki, SiHa and C33A, respectively. However, when cells were pre-treated with INI-43, a significant dose-dependent decrease in cisplatin IC<sub>50</sub> was observed in both HeLa and SiHa cells (44% and 46% in HeLa and SiHa cells, respectively) (Fig. 1.A). A small reduction in cisplatin IC<sub>50</sub> was observed in CaSki cells and no change in cisplatin IC<sub>50</sub> observed in C33A cells.

Cell viability was next examined at fixed cisplatin concentrations, with or without INI-43 pre-treatment. Figure 1.B shows that in HeLa, CaSki and SiHa cells, CT resulted in significantly decreased cell viability compared to their cisplatin-only treated counterparts. In line with the cisplatin IC<sub>50</sub> results, C33A showed no change in cell viability after single or CT. As 5  $\mu$ M INI-43 on its own did not affect cell viability across all cell lines, this suggests that the enhanced cell death observed in the CT was due to the combined action of INI-43 and cisplatin, rather than addition of independent effects of the two drugs.

To determine whether INI-43-cisplatin CT resulted in increased apoptosis, PARP cleavage and caspase-3/7 activation were assayed. Protein from live and dead cells was collected and PARP status examined by western blot. In both HeLa and SiHa cells, enhanced PARP cleavage was observed in the combination treated cells compared to those receiving cisplatin only (Fig. 1.C). Supporting the cell viability data, 5  $\mu$ M INI-43 treatment on its own showed negligible apoptosis. Investigation of caspase-3/7 activation revealed

that combination treated cells exhibited increased caspase-3/7 activation compared to cisplatin only treated cells (3.6-fold and 2.8-fold increase in HeLa cells and SiHa cells, respectively) (Fig. 1.D). These results suggest that nuclear import inhibition via INI-43 pre-treatment sensitized both HeLa and SiHa cells to cisplatin through enhanced activation of apoptosis.

INI-43 and cisplatin combination treatment resulted in synergistically enhanced cell death

Since the concentration of INI-43 used was not sufficient to induce significant cell death alone, and yet in combination with cisplatin it significantly enhanced cell death, it was proposed that INI-43 and cisplatin engaged in a synergistic interaction, where the cytotoxic effect of their combined use was greater than the additive effects of either drug used independently. To test this, the combination index (CI) was evaluated, according to the Chou-Talalay method, using a fixed dose ratio(25). SiHa cells were treated with INI-43 and cisplatin at varying concentrations to give INI-43-to-cisplatin ratios of 1:3, 1:4 or 1:5 (Table S1). Cells were pre-incubated with respective INI-43 concentrations for 2 hours prior to cisplatin treatment. Results showed that while cisplatin reduced cell viability in a dose-dependent manner, pre-treatment with INI-43 significantly enhanced this effect (Fig. 2.A). Based on the cell viability results, the CI values were calculated using CompuSyn software (ComboSyn, Inc.) and plotted against Fraction Affected (Fa), where  $Fa = 0$  and  $Fa = 1$  equates to no cell death and complete cell death, respectively. At  $Fa > 0.2$ , CI values were below 1 for INI-43 to cisplatin ratios of 1:3, 1:4 and 1:5, revealing synergistically enhanced cell death (Fig. 2.B).

Kpn $\beta$ 1 knock-down sensitized cervical cancer cells to cisplatin

To confirm that the enhancing effect of INI-43 on cisplatin cytotoxicity was due specifically to nuclear import inhibition, rather than off-target effects, cisplatin sensitivity was examined in Kpn $\beta$ 1 knock-down cells. Cells were transfected with Kpn $\beta$ 1 targeting siRNA (si-Kpn $\beta$ 1) or control siRNA (si-ctrl), and cisplatin sensitivity determined. Successful Kpn $\beta$ 1 knock-down was confirmed by western blotting 48 hours post transfection, at which point cisplatin treatment began (Fig. 3.A). In Kpn $\beta$ 1 knock-down cells, there was a significant reduction of cisplatin IC<sub>50</sub> from 24.4  $\mu$ M in the control cells to 9.7  $\mu$ M in HeLa cells, and 30.5  $\mu$ M in the control cells to 19.3  $\mu$ M in SiHa cells (Fig. 3.B). To confirm this effect, cell viability was measured after cisplatin treatment in Kpn $\beta$ 1 knock-down and control siRNA transfected cells. To eliminate the cell death that was caused by Kpn $\beta$ 1 knock-down, cell viability was normalized to untreated cells in each transfection group. Results indicated that Kpn $\beta$ 1 knock-down cells were more sensitive to cisplatin-induced cell death at all concentrations tested (Fig. 3.C). Furthermore, Kpn $\beta$ 1 knock-down HeLa and SiHa cells exhibited visibly increased PARP cleavage after cisplatin treatment compared to control siRNA-transfected cisplatin-treated cells (Fig. 3.D). Collectively, these results show that Kpn $\beta$ 1 knock-down enhanced sensitivity to cisplatin, similarly to that observed after INI-43 treatment, supporting that INI-43 increases cisplatin sensitivity by disrupting Kpn $\beta$ 1 function.

p53 is an important mediator of INI-43-cisplatin-induced cell death

To elucidate whether p53 might play a role in the cellular response to cisplatin and furthermore, whether the enhanced cisplatin sensitivity in INI-43 pre-treated cells involved p53, the effects of p53 knock-down were examined. p53 knock-down was confirmed via western blot 48 hours post transfection, at which point cells were subjected to drug treatments as previously described (Fig. 4.A). After single cisplatin treatment, p53 knock-down cells exhibited similar cell viability to si-ctrl transfected cells, suggesting that p53 was not involved in cisplatin-induced cell death (Fig. 4.B). These results were validated by PARP cleavage analysis, where similar levels of cleaved PARP were observed between the control and p53 knock-down cells at the same cisplatin concentrations (Fig. 4.C).

The impact of p53 on the enhancement of cell death observed after INI-43 and cisplatin CT was next examined. To quantify the "additional" cell death associated with the CT, cell viability was normalized to single cisplatin treatment. As previously established, a significant reduction in cell viability was observed after INI-43 and cisplatin CT, compared to single cisplatin treatment in the si-ctrl transfected cells. However, p53 knock-down cells exhibited similar sensitivity to single and CT, i.e, INI-43 pre-treatment induced sensitisation to cisplatin was lost with p53 inhibition (Fig. 4.D). Examination of PARP cleavage in these cells showed similar results; while si-ctrl transfected cells showed increased levels of cleaved PARP after CT compared to single cisplatin treatment, p53 knock-down cells exhibited similar levels of cleaved PARP between single and CT (Fig. 4.E). These results showed that cisplatin alone induced cell death is p53-independent, however, p53 appears to be critical for the enhancement of cell death observed in the CT, as p53 knock-down abrogated this effect.

#### INI-43 pre-treatment stabilized p53 via Kpn $\beta$ 1 inhibition

p53 is known to be highly unstable in HPV positive cells due to the activity of HPV oncoprotein E6(27), and as SiHa is an HPV 16 positive cell line known to express E6(28), it was possible that INI-43 treatment interfered with p53 stability, thereby altering cell sensitivity to cisplatin treatment. To test this, the rate of p53 degradation was monitored in cycloheximide (CHX)-treated cells. Cells were treated with 5  $\mu$ M INI-43 or DMSO for 2 hours, whereafter CHX was added and protein extracted at various time points after CHX treatment. Western blot analysis showed an increase in p53 stability in INI-43 treated cells compared to DMSO treated control cells (Fig. 5.A). To confirm that the prolonged p53 presence observed after INI-43 treatment was associated with Kpn $\beta$ 1 inhibition, p53 levels were also examined in Kpn $\beta$ 1 knock-down cells after CHX treatment. Similar to that observed after INI-43 treatment, Kpn $\beta$ 1 knock-down cells were able to sustain p53 for a longer period after CHX treatment (Fig. 5.B). The half-life of p53 was calculated and an approximate 2.9-fold and 3.7-fold increase in half-life was observed, in INI-43 treated and si-Kpn $\beta$ 1 transfected cells, respectively, compared to control cells (Fig. 5.C). Similar observations were made in HeLa cells, where Kpn $\beta$ 1 knock-down increased p53 half-life by approximately 3.3-fold (data not shown). To investigate whether the stabilization of p53 had any functional relevance, p53 reporter activity was measured after INI-43 treatment. 5  $\mu$ M INI-43 treatment led to a small but significant increase in p53 activity, consistent with its prolonged half-life (Fig. 5.D).

To relate these findings to combination treated cells, p53 reporter activity was measured in SiHa cells treated with INI-43 and cisplatin, compared to single cisplatin treatment. Interestingly, p53 reporter activity was significantly reduced upon single cisplatin treatment, in line with the lack of involvement of p53 in cisplatin-induced cell death observed in Fig. 4 (Fig. 5.E). However, with INI-43 pre-treatment, p53 reporter activity was significantly increased (Fig. 5.E). Following from the increased p53 reporter activity, the levels of two proteins known to be regulated by p53 were investigated: p21 which is positively regulated by p53, and Mcl-1 which is transcriptionally repressed by p53. Western blot analysis showed that cisplatin treatment at 30  $\mu$ M and 60  $\mu$ M decreased levels of both p21 and Mcl-1. However, in cells receiving both INI-43 and cisplatin, p21 levels were elevated compared to single cisplatin treatment at both 30 and 60  $\mu$ M concentrations, and Mcl-1 levels were reduced at 60  $\mu$ M cisplatin (Fig. 5.F). These results confirm the involvement of p53 and p53 downstream targets in the INI-43-mediated enhanced cytotoxicity to cisplatin.

INI-43-cisplatin combination treatment reduced cisplatin-induced nuclear accumulation of NF $\kappa$ B

We have previously shown that treating cancer cells with INI-43 prohibited PMA-stimulated nuclear entry of NF $\kappa$ B-p65(11). Others have reported that in SiHa cells, cisplatin treatment leads to activation of NF $\kappa$ B which contributes to cisplatin resistance in various cancer models(29). As NF $\kappa$ B activation requires nuclear translocation to initiate transcription of downstream targets, NF $\kappa$ B nuclear localization was evaluated by immunofluorescence after single and CT, as an indication of activity. Results showed that while cisplatin treatment stimulated nuclear localization of NF $\kappa$ B-p50 and NF $\kappa$ B-p65, INI-43 pre-treatment prevented this nuclear translocation of both NF $\kappa$ B subunits upon cisplatin treatment (Fig. 6.A and C). Fluorescence quantification supported these results, where cisplatin treatment led to a significant increase in nuclear fluorescence relative to cytoplasmic fluorescence (Fc(Nu/Cy)), and the INI-43-cisplatin CT significantly reduced this effect (Fig. 6.B and D).

To independently confirm these results, nuclear and cytoplasmic protein fractions were isolated from cisplatin-treated or combination treated SiHa cells. Western blot analysis showed that cisplatin treatment resulted in increased levels of both NF $\kappa$ B-p50 and NF $\kappa$ B-p65 in the nucleus, and that INI-43-cisplatin CT reduced this effect (Fig. 6.E). Next, it was determined whether the altered localization of NF $\kappa$ B-p50 and NF $\kappa$ B-p65 after CT translated into functional significance. p65 reporter activity was measured after single or CT, and results showed that p65 reporter activity was induced upon cisplatin treatment, but the increase in p65 activity was reduced when cells were pre-treated with INI-43 (Fig. 6.F). The expression of three downstream targets of NF $\kappa$ B known to respond to cisplatin treatment were hence examined, namely cyclin D1, c-Myc and X Chromosome Linked Inhibitor of Apoptosis (XIAP)(30–32). Western blot analysis showed that single cisplatin treatment led to elevated levels of cyclin D1 and c-Myc (Fig. 6.G). Moreover, the levels of cyclin D1, c-Myc and XIAP were all reduced in INI-43-cisplatin combination treated cells in a concentration dependent manner compared to single cisplatin treated cells (Fig. 6.G). As both cyclin D1 and c-Myc have been shown to confer chemoresistance via increasing the cells' DNA repair capacity(33, 34), we examined whether their decreased levels observed in the CT had an impact on cisplatin-induced DNA damage. The level of phosphorylated Histone 2AX ( $\gamma$ H2AX), a marker for DNA damage was

examined 24 hours after single or CT by western blot. Results showed that the INI-43-cisplatin CT increased  $\gamma$ H2AX levels in a concentration dependent manner, suggesting that pre-treating cells with INI-43 prior to cisplatin treatment enhanced the DNA damaging effect of cisplatin (Fig. 6.G).

Together, these results demonstrate that INI-43 pre-treatment effectively reduced nuclear accumulation and activity of NF $\kappa$ B, resulting in decreased expression of cyclin D1, c-Myc and XIAP, and impaired DNA repair ability, sensitising the cells to cisplatin treatment.

## Discussion

This study is a first to demonstrate that inhibition of Kpn $\beta$ 1 is an effective way to enhance the anti-cancer effects of cisplatin, and that both cisplatin sensitive, HeLa, and the more resistant, SiHa cervical cancer cells were responsive to this treatment. Furthermore, combination index analysis indicated a synergistic interaction between INI-43 and cisplatin, where their combined use produced greater anti-cancer effects compared to the added effects when used alone.

To understand the mechanism of action underlying the increased cisplatin sensitivity observed in the CT, proteins involved in cisplatin response were investigated, including both p53 and NF $\kappa$ B. Whilst p53 is widely accepted as a tumour suppressor protein important in guarding the genome and regulating apoptosis, some evidence has emerged to demonstrate that p53 can also promote oncogenesis by preventing apoptosis(35), suggesting that p53 can be involved in cisplatin resistance or cisplatin-induced apoptosis. p53 knock-down experiments demonstrated that p53 is involved in the pro-apoptotic pathway in our model system, but only in response to the CT, as p53 knock-down did not affect sensitivity to single cisplatin treatment. It is possible that in response to single cisplatin treatment there is functional compensation by other p53 family members like p73 and p63 when p53 is knocked down using siRNA, but this remains to be determined.

However, in combination treated cells, there was increased p53 stability and activity after INI-43 pre-treatment, which associated with increased responsiveness to cisplatin treatment. SiHa is HPV positive, harbouring the HPV16 E6 oncoprotein(28), which has been reported to directly associate with p53 and induce its degradation(27). This results in a highly unstable p53, which is supported by our observation whereby p53 is rapidly degraded after CHX treatment. Stabilization of p53 has also been observed in HPV16 and HPV18 positive Kpn $\beta$ 1 knock-down CaSki cells(10), and interestingly, inhibition of CRM1 via small molecules KPT-185 and leptomycin B has also been shown to stabilize p53 in other cancers(36, 37). Together with our findings, these data suggest that interfering with the nuclear transport system in either directions has stabilizing effects on p53. It is likely that in our model system, p53 is rapidly degraded making the p53-associated apoptotic pathway less accessible to the cisplatin-induced DNA damage response, and thus p53 knock-down had little effect on cisplatin induced cell death. INI-43 pre-treatment moderately stabilized p53, thereby making p53 activity more readily available for apoptotic induction when cells are challenged with cisplatin. This could also explain why INI-43 did not sensitize C33A cells to cisplatin, as C33A cells carry a non-functional mutant p53(38).

In addition to enhanced p53 stability and reporter activity, increased p21 levels and decreased Mcl-1 levels were observed in INI-43 pre-treated cells compared to non-pre-treated cells in response to cisplatin treatment. p53 is known to positively regulate p21 expression and repress Mcl-1(39, 40). Furthermore, the elevated caspase-3/7 activity observed in the CT could be associated with the decreased levels of Mcl-1, as Mcl-1 is known to promote survival by inhibiting events preceding mitochondrial release of cytochrome C(41). Whilst the link between Kpn $\beta$ 1 inhibition and p53 stabilization is demonstrated in our results, further experiments should be performed to address how nuclear import inhibition leads to p53 stabilization, and whether this is mediated through interfering with HPV 16 E6 activity.

Interestingly, with opposing roles in apoptosis, NF $\kappa$ B and p53 have been shown to mutually antagonize the transcriptional activity of each other(42), and our results showed there was also a differential distribution of NF $\kappa$ B subunits p50 and p65 in cells receiving the single cisplatin and CT. NF $\kappa$ B is an important response factor to stress signals, including cisplatin-induced DNA damage(43), whereupon it relocates to the nucleus to promote the transcription of various genes involved in DNA repair and survival(29). As NF $\kappa$ B is reliant on Kpn $\beta$ 1/Karyopherin $\alpha$  for nuclear entry(44), the localisation of NF $\kappa$ B was measured after INI-43 treatment which showed that INI-43 inhibited cisplatin-induced nuclear import of NF $\kappa$ B, as well as the expression of its transcriptional targets cyclin D1, c-Myc and XIAP. This coincided with elevated levels of  $\gamma$ H2AX, suggesting that Kpn $\beta$ 1 inhibition either augmented the DNA damaging capacity of cisplatin, or, alternatively, impaired the DNA repair response. c-Myc confers chemoresistance via suppressing BIN1, an inhibitor of PARP-1 involved in DNA repair activity, thereby increasing tolerance to DNA damage and conferring cisplatin resistance(34). XIAP promotes survival by directly binding to and inhibiting the activities of caspase-3, caspase-7 and possibly caspase-9(45). Cyclin D1, best known for driving cell cycle from G1 to S phase, is also involved in DNA damage repair in association with Rad51(46), and its inhibition impairs DNA repair capacity leading to sensitization of cancer cells to cisplatin(33). Our results showed that INI-43-cisplatin CT results in reduced levels of these DNA-repair and anti-apoptotic proteins, possibly via decreasing NF $\kappa$ B nuclear import and transcriptional activity. However, it must also be noted that the response of these proteins to INI-43-cisplatin CT may also be attributed to other mechanisms besides NF $\kappa$ B. For example, Yang et al. (2019) recently showed that in addition to blocking NF $\kappa$ B nuclear translocation, Kpn $\beta$ 1 inhibition also reduced the nuclear translocation of c-Myc in prostate cancer cells(47).

## Conclusions

Taken together, this study shows that Kpn $\beta$ 1 inhibition sensitizes cervical cancer cells to cisplatin, suggesting that coupling nuclear import inhibition with cisplatin may be an effective anti-cancer approach. This is mediated through stabilisation of p53 and prevention of NF $\kappa$ B nuclear localization, leading to alterations in the expression of various downstream targets such as XIAP, c-Myc, and Mcl-1. These proteins are known to confer cisplatin resistance in a variety of cancers, and their inhibition through genetic or pharmacological approaches have been demonstrated to increase sensitivity to chemotherapeutic agents(32, 48, 49). The abrogation of enhanced cell death in combination treated cells via p53 knock-down suggest that p53 is likely upstream of the NF $\kappa$ B-induced survival response.

Interestingly, CRM1 inhibition via leptomycin B has similarly been demonstrated to enhance cisplatin sensitivity in p53 wildtype cervical cancer cells(50), suggesting that p53 may play a crucial role in the enhanced sensitivity of HPV positive cells to cisplatin after nuclear transport inhibition.

## Abbreviations

Kpn $\beta$ 1

Karyopherin beta 1

Crm1

Chromosome Region Maintenance 1

CT

combination treatment

IC<sub>50</sub>

half inhibitory concentration

CI

combination index

Fa

fraction affected

T<sub>1/2</sub>

half-life

CHX

cycloheximide

si-Kpn $\beta$ 1

Kpn $\beta$ 1-targeting siRNA

si-ctrl

control siRNA

Fc(Nu/Cy)

nuclear fluorescence relative to cytoplasmic fluorescence

XIAP

X-Chromosome Linked Inhibitor of Apoptosis

$\gamma$ H2AX

phosphorylated Histone 2AX

## Declarations

### Ethics approval and consent to participate

Not applicable

### Consent for publication

Not applicable

## Availability of data and materials

Data sharing is not applicable to this article as no datasets were generated or analysed during the current study.

## Competing interests

The authors declare they have no competing interests.

## Funding

This work was supported by grants obtained by VL from the South African Medical Research Council, the National Research Foundation, the Cancer Association of South Africa (CANSA), and the University of Cape Town. The funders had no role in the study design, data collection and analysis, decision to publish or preparation of the manuscript.

## Authors' contributions

AC and PvdW performed experiments. AC, PvdW, WW, MB and VL analysed and interpreted the data. AC wrote the manuscript, with editing from PvdW, WW and VL. VL supervised and obtained the research funding for the study. All authors read and approved the final manuscript.

## Acknowledgements

Not applicable

## References

1. van der Watt PJ, Maske CP, Hendricks DT, Parker MI, Denny L, Govender D, et al. The Karyopherin proteins, Crm1 and Karyopherin beta1, are overexpressed in cervical cancer and are critical for cancer cell survival and proliferation. *Int J Cancer*. 2009;124(8):1829–40.
2. Stelma T, Chi A, van der Watt PJ, Verrico A, Lavia P, Leaner VD. Targeting nuclear transporters in cancer: Diagnostic, prognostic and therapeutic potential. *IUBMB Life*. 2016;68(4):268–80.
3. Fornerod M, Ohno M, Yoshida M, Mattaj IW. CRM1 is an export receptor for leucine-rich nuclear export signals. *Cell*. 1997;90(6):1051–60.
4. Wang AY, Liu H. The past, present, and future of CRM1/XPO1 inhibitors. *Stem cell investigation*. 2019;6:6.
5. Chook YM, Suel KE. Nuclear import by karyopherin-betas: recognition and inhibition. *Biochim Biophys Acta*. 2011;1813(9):1593–606.
6. Ciciarello M, Mangiacasale R, Thibier C, Guarguaglini G, Marchetti E, Di Fiore B, et al. Importin beta is transported to spindle poles during mitosis and regulates Ran-dependent spindle assembly factors in

- mammalian cells. *J Cell Sci.* 2004;117(Pt 26):6511–22.
7. Schmitz MH, Held M, Janssens V, Hutchins JR, Hudecz O, Ivanova E, et al. Live-cell imaging RNAi screen identifies PP2A-B55alpha and importin-beta1 as key mitotic exit regulators in human cells. *Nat Cell Biol.* 2010;12(9):886–93.
  8. Kuusisto HV, Jans DA. Hyper-dependence of breast cancer cell types on the nuclear transporter Importin beta1. *Biochim Biophys Acta.* 2015;1853(8):1870–8.
  9. Martens-de Kemp SR, Nagel R, Stigter-van Walsum M, van der Meulen IH, van Beusechem VW, Braakhuis BJ, et al. Functional genetic screens identify genes essential for tumor cell survival in head and neck and lung cancer. *Clin Cancer Res.* 2013;19(8):1994–2003.
  10. Angus L, van der Watt PJ, Leaner VD. Inhibition of the nuclear transporter, Kpnbeta1, results in prolonged mitotic arrest and activation of the intrinsic apoptotic pathway in cervical cancer cells. *Carcinogenesis.* 2014;35(5):1121–31.
  11. van der Watt PJ, Chi A, Stelma T, Stowell C, Strydom E, Carden S, et al. Targeting the Nuclear Import Receptor Kpnbeta1 as an Anticancer Therapeutic. *Mol Cancer Ther.* 2016;15(4):560–73.
  12. Long HJ 3rd, Bundy BN, Grendys EC Jr, Benda JA, McMeekin DS, Sorosky J, et al. Randomized phase III trial of cisplatin with or without topotecan in carcinoma of the uterine cervix: a Gynecologic Oncology Group Study. *J Clin Oncol.* 2005;23(21):4626–33.
  13. Takekida S, Fujiwara K, Nagao S, Yamaguchi S, Yoshida N, Kitada F, et al. Phase II study of combination chemotherapy with docetaxel and carboplatin for locally advanced or recurrent cervical cancer. *International journal of gynecological cancer: official journal of the International Gynecological Cancer Society.* 2010;20(9):1563–8.
  14. Tsuda H, Hashiguchi Y, Nishimura S, Miyama M, Nakata S, Kawamura N, et al. Phase I-II study of irinotecan (CPT-11) plus nedaplatin (254-S) with recombinant human granulocyte colony-stimulating factor support in patients with advanced or recurrent cervical cancer. *Br J Cancer.* 2004;91(6):1032–7.
  15. Burnett AF, Roman LD, Garcia AA, Muderspach LI, Brader KR, Morrow CP. A phase II study of gemcitabine and cisplatin in patients with advanced, persistent, or recurrent squamous cell carcinoma of the cervix. *Gynecol Oncol.* 2000;76(1):63–6.
  16. Sahin K, Tuzcu M, Basak N, Caglayan B, Kilic U, Sahin F, et al. Sensitization of Cervical Cancer Cells to Cisplatin by Genistein: The Role of NFkappaB and Akt/mTOR Signaling Pathways. *J Oncol.* 2012;2012:461562.
  17. Pariente R, Pariente JA, Rodriguez AB, Espino J. Melatonin sensitizes human cervical cancer HeLa cells to cisplatin-induced cytotoxicity and apoptosis: effects on oxidative stress and DNA fragmentation. *Journal of pineal research.* 2016;60(1):55–64.
  18. Kilic U, Sahin K, Tuzcu M, Basak N, Orhan C, Elibol-Can B, et al. Enhancement of Cisplatin sensitivity in human cervical cancer: epigallocatechin-3-gallate. *Frontiers in nutrition.* 2014;1:28.
  19. Zhu J, Wang Y, Huang H, Yang Q, Cai J, Wang Q, et al. Upregulation of KPNbeta1 in gastric cancer cell promotes tumor cell proliferation and predicts poor prognosis. *Tumour Biol.* 2016;37(1):661–72.

20. Carden S, van der Watt P, Chi A, Ajayi-Smith A, Hadley K, Leaner VD. A tight balance of Karyopherin  $\beta$ 1 expression is required in cervical cancer cells. *BMC Cancer*. 2018;18(1):1123.
21. Turner JG, Dawson J, Emmons MF, Cubitt CL, Kauffman M, Shacham S, et al. CRM1 Inhibition Sensitizes Drug Resistant Human Myeloma Cells to Topoisomerase II and Proteasome Inhibitors both In Vitro and Ex Vivo. *J Cancer*. 2013;4(8):614–25.
22. Salas Fragomeni RA, Chung HW, Landesman Y, Senapedis W, Saint-Martin JR, Tsao H, et al. CRM1 and BRAF inhibition synergize and induce tumor regression in BRAF-mutant melanoma. *Mol Cancer Ther*. 2013;12(7):1171–9.
23. Gong LH, Chen XX, Wang H, Jiang QW, Pan SS, Qiu JG, et al. Piperlongumine induces apoptosis and synergizes with cisplatin or paclitaxel in human ovarian cancer cells. *Oxid Med Cell Longev*. 2014;2014:906804.
24. Kashyap T, Argueta C, Unger T, Klebanov B, Debler S, Senapedis W, et al. Selinexor reduces the expression of DNA damage repair proteins and sensitizes cancer cells to DNA damaging agents. *Oncotarget*. 2018;9(56):30773–86.
25. Chou TC, Talalay P. Quantitative analysis of dose-effect relationships: the combined effects of multiple drugs or enzyme inhibitors. *Adv Enzyme Regul*. 1984;22:27–55.
26. el-Deiry WS, Tokino T, Velculescu VE, Levy DB, Parsons R, Trent JM, et al. WAF1, a potential mediator of p53 tumor suppression. *Cell*. 1993;75(4):817–25.
27. Crook T, Tidy JA, Vousden KH. Degradation of p53 can be targeted by HPV E6 sequences distinct from those required for p53 binding and trans-activation. *Cell*. 1991;67(3):547–56.
28. Meissner JD. Nucleotide sequences and further characterization of human papillomavirus DNA present in the CaSki, SiHa and HeLa cervical carcinoma cell lines. *J Gen Virol*. 1999;80(Pt 7):1725–33.
29. Godwin P, Baird AM, Heavey S, Barr MP, O'Byrne KJ, Gately K. Targeting nuclear factor-kappa B to overcome resistance to chemotherapy. *Front Oncol*. 2013;3:120.
30. Basu A, Krishnamurthy S. Cellular responses to Cisplatin-induced DNA damage. *J Nucleic Acids*. 2010;2010.
31. Zhou X, Zhang Z, Yang X, Chen W, Zhang P. Inhibition of cyclin D1 expression by cyclin D1 shRNAs in human oral squamous cell carcinoma cells is associated with increased cisplatin chemosensitivity. *Int J Cancer*. 2009;124(2):483–9.
32. Xu B, Liu P, Li J, Lu H. c-MYC depletion potentiates cisplatin-induced apoptosis in head and neck squamous cell carcinoma: involvement of TSP-1 up-regulation. *Ann Oncol*. 2010;21(3):670–2.
33. Jirawatnotai S, Hu Y, Livingston DM, Sicinski P. Proteomic identification of a direct role for cyclin d1 in DNA damage repair. *Cancer Res*. 2012;72(17):4289–93.
34. Pyndiah S, Tanida S, Ahmed KM, Cassimere EK, Choe C, Sakamuro D. c-MYC suppresses BIN1 to release poly(ADP-ribose) polymerase 1: a mechanism by which cancer cells acquire cisplatin resistance. *Sci Signal*. 2011;4(166):ra19.

35. Janicke RU, Sohn D, Schulze-Osthoff K. The dark side of a tumor suppressor: anti-apoptotic p53. *Cell Death Differ.* 2008;15(6):959–76.
36. Wang S, Han X, Wang J, Yao J, Shi Y. Antitumor effects of a novel chromosome region maintenance 1 (CRM1) inhibitor on non-small cell lung cancer cells in vitro and in mouse tumor xenografts. *PLoS One.* 2014;9(3):e89848.
37. Lecane PS, Kiviharju TM, Sellers RG, Peehl DM. Leptomycin B stabilizes and activates p53 in primary prostatic epithelial cells and induces apoptosis in the LNCaP cell line. *Prostate.* 2003;54(4):258–67.
38. Crook T, Wrede D, Vousden KH. p53 point mutation in HPV negative human cervical carcinoma cell lines. *Oncogene.* 1991;6(5):873–5.
39. He G, Siddik ZH, Huang Z, Wang R, Koomen J, Kobayashi R, et al. Induction of p21 by p53 following DNA damage inhibits both Cdk4 and Cdk2 activities. *Oncogene.* 2005;24(18):2929–43.
40. Pietrzak M, Puzianowska-Kuznicka M. p53-dependent repression of the human MCL-1 gene encoding an anti-apoptotic member of the BCL-2 family: the role of Sp1 and of basic transcription factor binding sites in the MCL-1 promoter. *Biological chemistry.* 2008;389(4):383–93.
41. Clohessy JG, Zhuang J, de Boer J, Gil-Gomez G, Brady HJ. Mcl-1 interacts with truncated Bid and inhibits its induction of cytochrome c release and its role in receptor-mediated apoptosis. *J Biol Chem.* 2006;281(9):5750–9.
42. Webster GA, Perkins ND. Transcriptional cross talk between NF-kappaB and p53. *Mol Cell Biol.* 1999;19(5):3485–95.
43. Volcic M, Karl S, Baumann B, Salles D, Daniel P, Fulda S, et al. NF-kappaB regulates DNA double-strand break repair in conjunction with BRCA1-CtIP complexes. *Nucleic acids research.* 2012;40(1):181–95.
44. Yan W, Li R, He J, Du J, Hou J. Importin beta1 mediates nuclear factor-kappaB signal transduction into the nuclei of myeloma cells and affects their proliferation and apoptosis. *Cell Signal.* 2015;27(4):851–9.
45. Salvesen GS, Duckett CS. IAP proteins: blocking the road to death's door. *Nature reviews Molecular cell biology.* 2002;3(6):401–10.
46. Jirawatnotai S, Hu Y, Michowski W, Elias JE, Becks L, Bienvenu F, et al. A function for cyclin D1 in DNA repair uncovered by protein interactome analyses in human cancers. *Nature.* 2011;474(7350):230–4.
47. Yang J, Guo Y, Lu C, Zhang R, Wang Y, Luo L, et al. Inhibition of Karyopherin beta 1 suppresses prostate cancer growth. *Oncogene.* 2019;38(24):4700–14.
48. Dean EJ, Ward T, Pinilla C, Houghten R, Welsh K, Makin G, et al. A small molecule inhibitor of XIAP induces apoptosis and synergises with vinorelbine and cisplatin in NSCLC. *Br J Cancer.* 2010;102(1):97–103.
49. You L, Wang Y, Jin Y, Qian W. Downregulation of Mcl-1 synergizes the apoptotic response to combined treatment with cisplatin and a novel fiber chimeric oncolytic adenovirus. *Oncol Rep.* 2012;27(4):971–8.

50. Naniwa J, Kigawa J, Akesima R, Kanamori Y, Itamochi H, Oishi T, et al. Leptomycin B enhances CDDP-sensitivity via nuclear accumulation of p53 protein in HPV-positive cells. *Cancer Sci.* 2003;94(12):1099–103.

## Figures

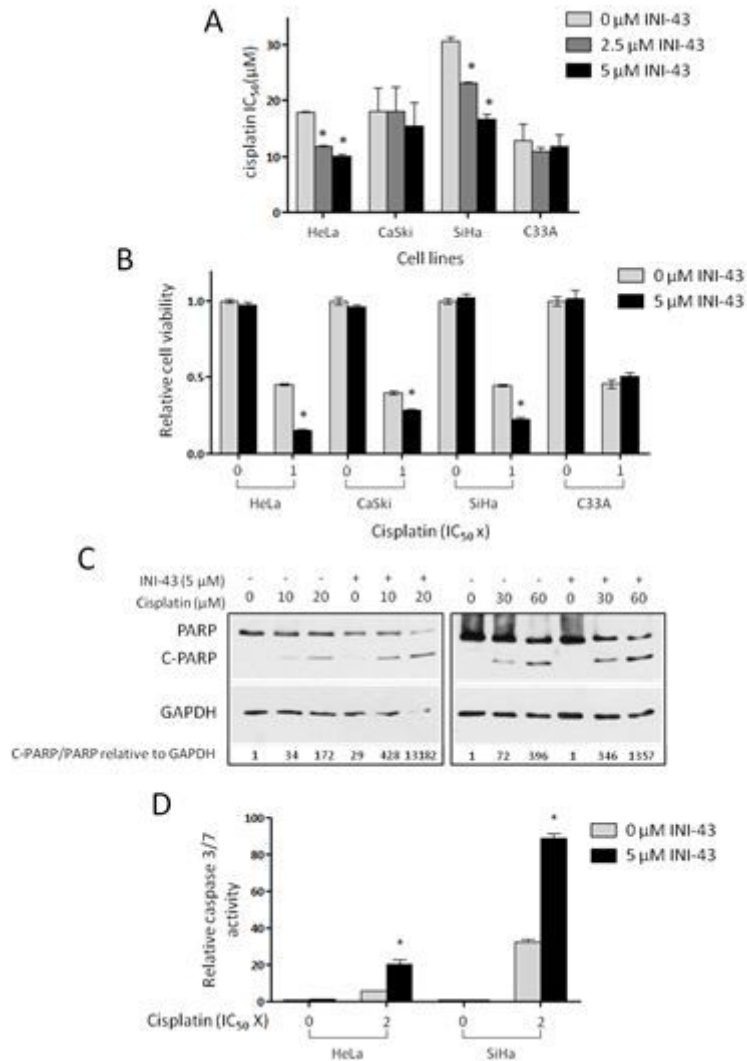


**Figure 1**

INI-43 pre-treatment significantly enhances cisplatin sensitivity in cervical cancer cell lines HeLa and SiHa. (A) Cisplatin IC<sub>50</sub> values in cervical cancer cell lines HeLa, CaSki, SiHa and C33A pre-treated with 2.5 μM and 5 μM INI-43 for 2 hours, compared to control cells receiving no pre-treatment. Results shown are the mean IC<sub>50</sub> value ± SEM of three independent experiments (n = 6). (B) MTT cell proliferation assay 48 hours post-treatment, showing increased cisplatin sensitivity in HeLa, CaSki and SiHa cells after pre-treatment with 5 μM INI-43. (C) Western blot analysis showing enhanced PARP cleavage in INI-43 and cisplatin combination treated HeLa and SiHa cells. GAPDH was used as a loading control, and

quantification via densitometry is shown. (D) Caspase-3/7 activity in HeLa and SiHa cells was significantly enhanced upon INI-43 and cisplatin combination treatment, compared to cisplatin single treatment. In all cases, results shown are the mean  $\pm$  SEM of experiments performed in triplicate and repeated three independent times (\* $p < 0.05$ ).

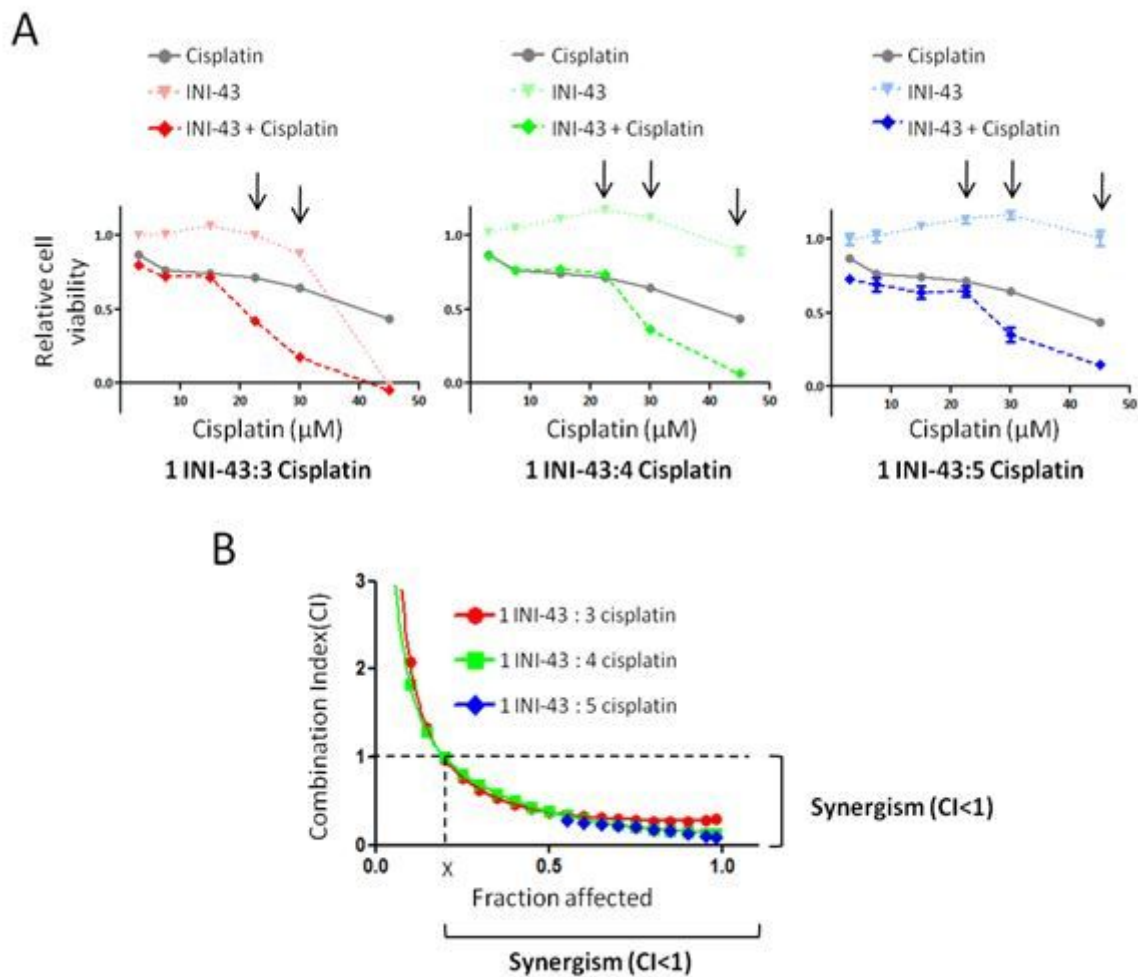


**Figure 2**

Combination index (CI) evaluation shows that INI-43 and cisplatin combination treatment results in a synergistic anti-cancer effect in SiHa cells. (A) Cells were subjected to INI-43, cisplatin or the combination treatment for 48 hours. Combination treatments were carried out at fixed INI-43-to-cisplatin ratios of 1:3, 1:4 and 1:5 (see Table S1). Viable cells were determined using the MTT assay and expressed relative to untreated. Arrows indicate enhanced cell death. (B) CI values were calculated using CompuSyn software and plotted against the fraction affected. Data shown are the mean  $\pm$  SEM ( $n = 5$ ) and experiments were repeated at least two independent times.

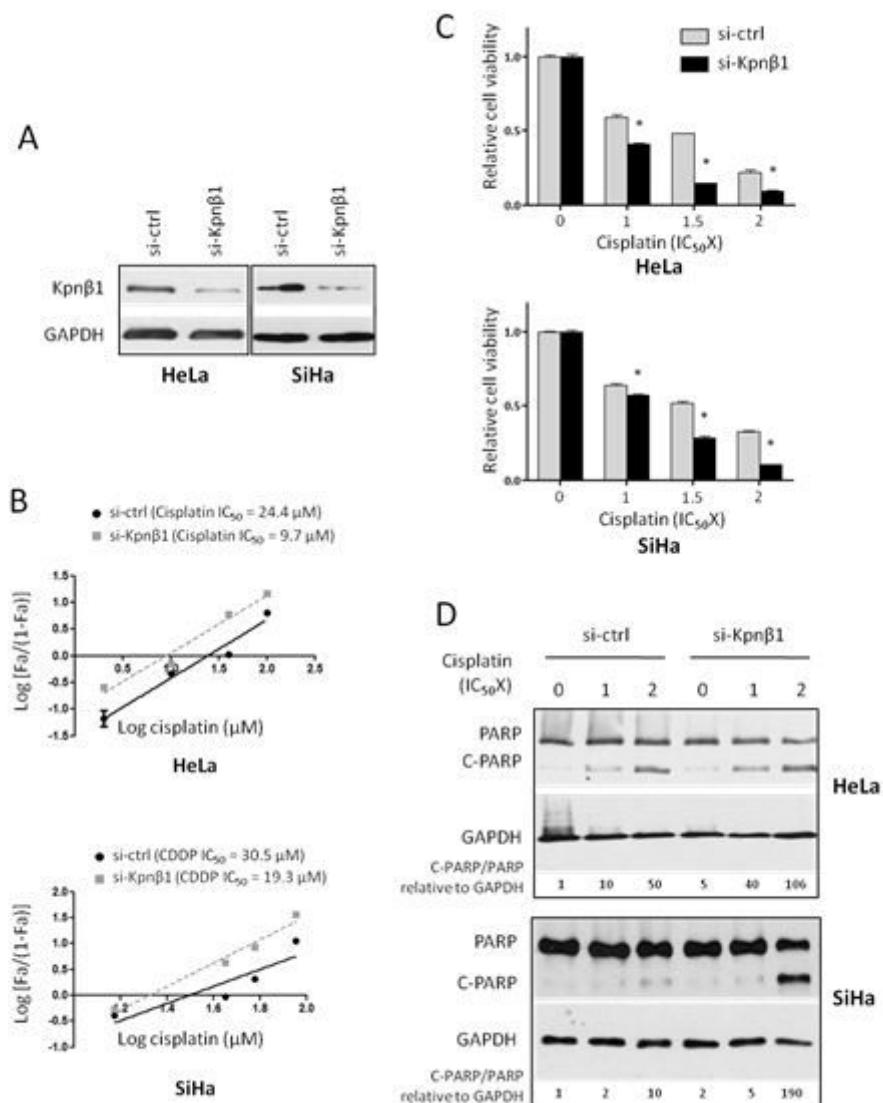


**Figure 3**

Kpnβ1 knock-down enhances cisplatin sensitivity in cervical cancer cells. (A) HeLa and SiHa cells were transfected with siRNA for 48 hours, after which Kpnβ1 knock-down was confirmed by western blotting, with GAPDH as the loading control. (B) Cisplatin IC<sub>50</sub> values were determined in Kpnβ1 knock-down HeLa and SiHa cells and results showed a decrease in cisplatin IC<sub>50</sub> in both cell lines when transfected with si-Kpnβ1 compared to si-ctrl. Data shown are results ± SEM (n = 6) of a representative experiment performed two times. (C) Kpnβ1 knock-down affected cell viability in response to cisplatin treatment in HeLa and SiHa cells. Control and Kpnβ1 knock-down cells were treated with cisplatin for 48 hours before viable cells were measured using the MTT assay. Data shown are mean ± SEM (n = 6) of one representative experiment repeated two times (\*p < 0.05). (D) Western blot showing that Kpnβ1 knock-down increased PARP cleavage after cisplatin treatment in HeLa and SiHa cells. GAPDH was included as a loading control, and densitometrical quantification of C-PARP/PARP relative to GAPDH is shown. Results are representative of experiments performed two independent times.

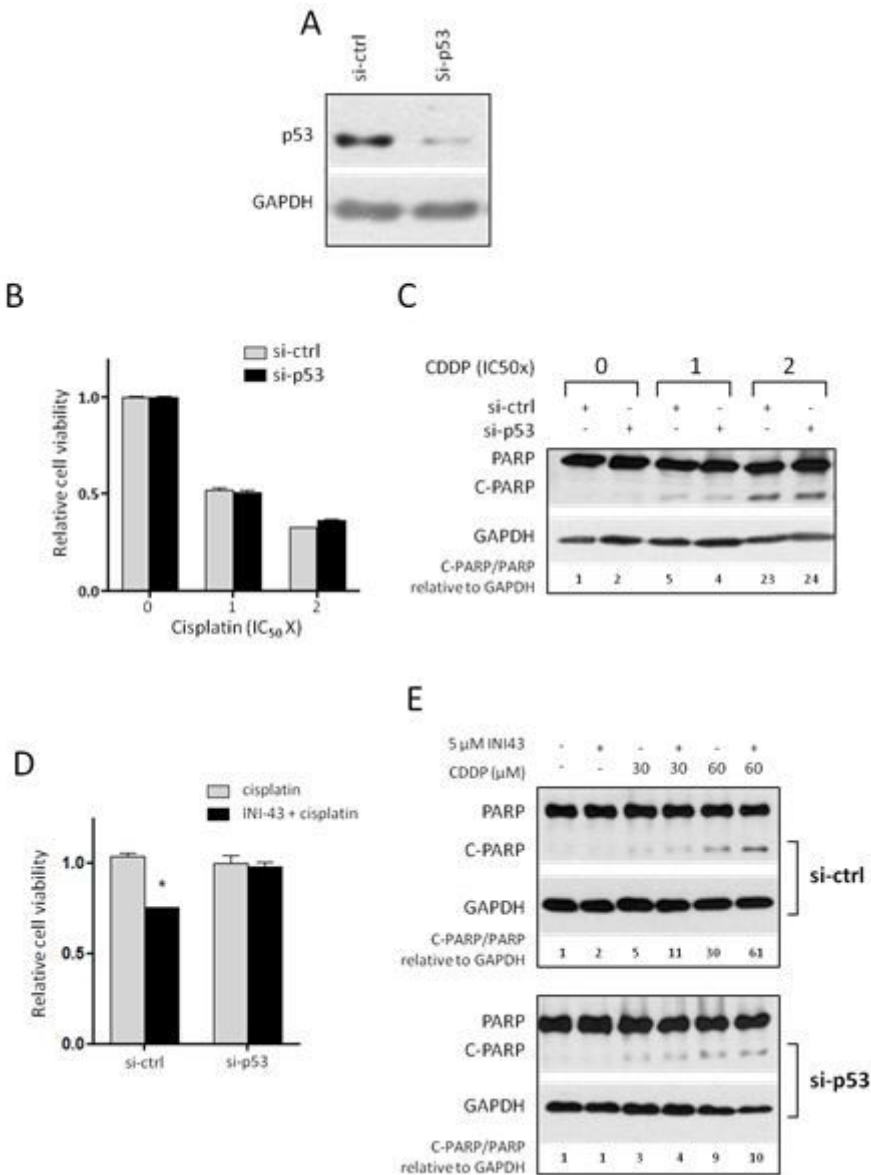


**Figure 4**

p53 inhibition does not affect cisplatin sensitivity but is required for the enhanced cell death observed in the combination treatment. (A) SiHa cells were transfected with siRNA for 48 hours and p53 knock-down confirmed via western blot. GAPDH was included as a loading control. (B) MTT assay showing that p53 knock-down does not affect cell viability after 48-hour cisplatin treatment. Data shown are the mean  $\pm$  SEM of experiments performed in triplicate and repeated two independent times. (C) Western blot showing that p53 knock-down does not affect cisplatin-induced PARP cleavage in SiHa cells. GAPDH was included as loading control, and densitometrical quantification is presented. Results shown are representative of experiments performed three times. (D) MTT assay comparing cell viability between single cisplatin treatment and INI-43-cisplatin combination treatment, in p53 knock-down SiHa cells. To compare the degree of enhancement of cell death as a result of the combination treatment, cell viability was normalized to cells receiving single cisplatin treatment. Results shown are mean  $\pm$  SEM of experiments performed in triplicate and repeated two independent times (\* $p < 0.05$ ). (E) Western blot

showing that p53 knock-down abrogated the enhancement of PARP cleavage observed after combination treatment compared to single cisplatin treatment. GAPDH was included as the loading control, and densitometrical quantification is shown. Results shown are representative of three independent experiments.

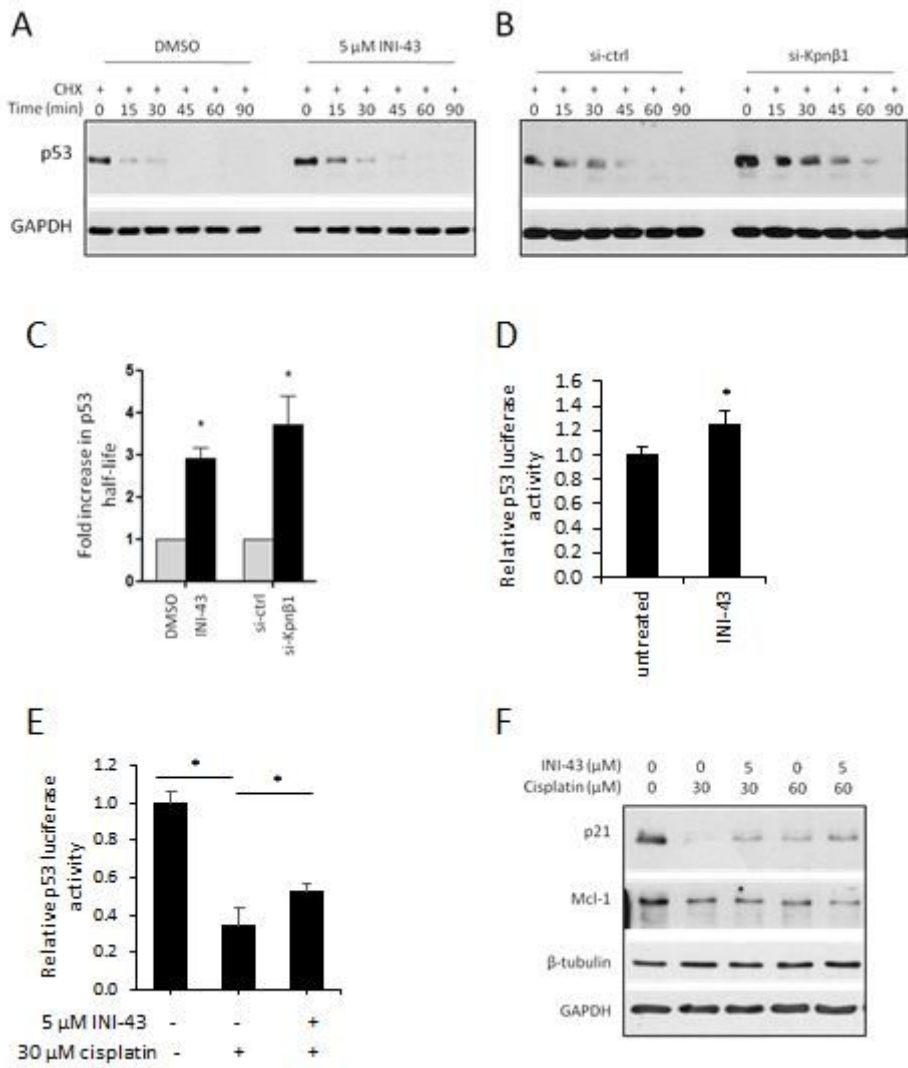


**Figure 5**

Inhibition of Kpn $\beta$ 1 results in increased p53 stability and reporter activity, as well as increased p21 and decreased Mcl-1 in response to cisplatin. (A, B) SiHa cells were treated with DMSO or 5  $\mu$ M INI-43 for 2 hours (A) or transfected with si-ctrl or si-Kpn $\beta$ 1 for 48 hours (B) followed by 50  $\mu$ g/mL CHX treatment. Protein was harvested at the indicated time points, and p53 content analyzed by western blot. GAPDH served as the loading control. (C) The fold increase in p53 half-life is shown as the mean  $\pm$  SEM from the three independent experiments (\*p < 0.05). (D) p53 reporter activity is increased upon 24 hours 5  $\mu$ M INI-43 treatment of SiHa cells (\*p < 0.05). Experiments were performed in triplicate and repeated at least three independent times. (E) p53 reporter activity is enhanced in INI-43-cisplatin combination treated SiHa cells, compared to cells treated with cisplatin alone (\*p < 0.05). Experiments were performed in triplicate and repeated at least three independent times. (F) Western blot showing levels of p53 targets p21 and

Mcl-1 after single and combination treatment.  $\beta$ -tubulin served as a loading control for Mcl-1 and GAPDH for p21. Results shown are representative of two independent experiments.

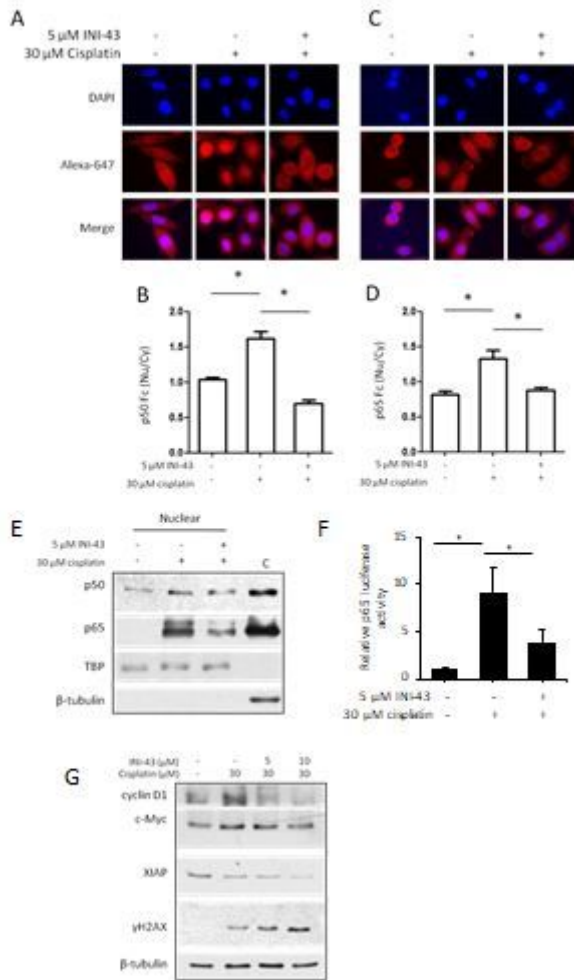


**Figure 6**

INI-43 pre-treatment reduces the nuclear localization of NF $\kappa$ B and expression of its targets and enhances DNA damage after cisplatin treatment in SiHa cells. (A, C) Distribution of NF $\kappa$ B subunits p50 (A) and p65 (C) were analyzed by immunofluorescence after single (30  $\mu$ M cisplatin) or combination treatment. (B, D) Fluorescence intensities were quantified using ImageJ and expressed as nuclear fluorescence relative to cytoplasmic fluorescence (Fc(Nu/Cy)) for p50 (B) and p65 (D). Results shown are representative images for each condition (A, C), and mean  $\pm$  SEM of 6 cells (\* $p < 0.05$ , B, D). (E) Western blot analysis showing increased nuclear p50 and p65 levels after cisplatin treatment, which was reduced if cells were pre-treated with INI-43. TBP served as the nuclear loading control and  $\beta$ -tubulin to confirm that pure nuclear lysates were obtained in comparison to a random cytoplasmic protein sample 'C'. Results shown are representative of experiments conducted three independent times. (F) p65 reporter assay showing increased p65 luciferase activity after 30  $\mu$ M single cisplatin treatment, which was reduced with INI-43 pre-treatment (\* $p < 0.05$ ). (G) Western blot showing changing levels of various NF $\kappa$ B targets (cyclin D1, c-Myc and XIAP) after single or combination treatment, and enhanced phosphorylation of H2A.X ( $\gamma$ H2AX)

in combination treated cells, indicative of increased DNA damage.  $\beta$ -tubulin was included as the loading control, and results shown are representative of experiments performed at least two independent times.

## Supplementary Files

This is a list of supplementary files associated with this preprint. Click to download.

- [SupplementaryfulllengthWesterns18Sept2020.pptx](#)
- [SupplementaryTableS1.docx](#)